CellPress

Neuron
Article

Subdomain-Mediated Axon-Axon Signaling and Chemoattraction Cooperate to Regulate Afferent Innervation of the Lateral Habenula

Ewoud Roberto Eduard Schmidt,[1,6] Sara Brignani,[1] Youri Adolfs,[1] Suzanne Lemstra,[1] Jeroen Demmers,[2] Marina Vidaki,[3] Amber-Lee Skye Donahoo,[4] Kersti Lilleväli,[5] Eero Vasar,[5] Linda Jane Richards,[4] Domna Karagogeos,[3] Sharon Margriet Kolk,[1,7] and Ronald Jeroen Pasterkamp[1,*]

[1]Department of Translational Neuroscience, Brain Center Rudolf Magnus, University Medical Center Utrecht, Universiteitsweg 100, 3584 CG Utrecht, the Netherlands

[2]Proteomics Centre and Department of Cell Biology, Erasmus University Medical Centre, Dr Molewaterplein 50, 3015 GE Rotterdam, the Netherlands

[3]Department of Basic Science, Faculty of Medicine, University of Crete and Institute of Molecular Biology and Biotechnology, Vassilika Vouton, Heraklion GR-7110, Greece

[4]Queensland Brain Institute and The School of Biomedical Sciences, University of Queensland, Building 79, St Lucia Campus, Brisbane, QLD 4067, Australia

[5]Department of Physiology, Institute of Biomedicine and Translational Medicine, University of Tartu, Ravila 19, 50411 Tartu, Estonia

[6]Present address: Department of Neuroscience, College of Physicians and Surgeons, Columbia University, 630 West 168th Street, New York, NY 10032, USA

[7]Present address: Department of Molecular Animal Physiology, Donders Institute for Brain, Cognition and Behaviour, Radboud University Nijmegen, Geert Grooteplein Zuid 28, 6525 GA Nijmegen, the Netherlands

*Correspondence: r.j.pasterkamp@umcutrecht.nl

http://dx.doi.org/10.1016/j.neuron.2014.05.036

SUMMARY

A dominant feature of neural circuitry is the organization of neuronal projections and synapses into specific brain nuclei or laminae. Lamina-specific connectivity is controlled by the selective expression of extracellular guidance and adhesion molecules in the target field. However, how (sub)nucleus-specific connections are established and whether axon-derived cues contribute to subdomain targeting are largely unknown. Here, we demonstrate that the lateral subnucleus of the habenula (lHb) determines its own afferent innervation by sending out efferent projections that express the cell adhesion molecule LAMP to reciprocally collect and guide dopaminergic afferents to the lHb—a phenomenon we term subdomain-mediated axon-axon signaling. This process of reciprocal axon-axon interactions cooperates with lHb-specific chemoattraction mediated by Netrin-1, which controls axon target entry, to ensure specific innervation of the lHb. We propose that cooperation between pretarget reciprocal axon-axon signaling and subdomain-restricted instructive cues provides a highly precise and general mechanism to establish subdomain-specific neural circuitry.

INTRODUCTION

The formation of precise connections between afferent axons and their partner neurons is essential for the assembly of functional neural circuits. The organization of the nervous system in two main anatomical units, i.e., brain nuclei and laminated structures, facilitates this process by spatially grouping synaptic partners and enabling subdomain-restricted expression of instructive cues. Despite the important role of these organizing principles, our understanding of the cellular and molecular basis of lamina- or subnucleus-specific circuit development is still limited.

Our current knowledge of subdomain-specific axon targeting mainly derives from work on laminated structures, and recent studies have uncovered different molecular strategies that control lamina-specific targeting independent of neural activity. This work shows that initially target-derived, membrane-associated, or secreted guidance cues function to direct axon projections to or exclude them from specific layers. Subsequently, combinatorial expression of cell adhesion molecules facilitates the formation of contacts between matched pre- and postsynaptic neurons (Baier, 2013; Huberman et al., 2010; Robles and Baier, 2012; Sanes and Yamagata, 2009; Williams et al., 2010). Similar to laminated structures, brain nuclei are often subdivided into smaller subdomains comprising small clusters of related neurons (e.g., Aizawa et al., 2012; Molnár et al., 2012). A striking example of a brain nucleus in which subdomain-specific connectivity coordinates complex physiological functions is the habenula (Aizawa et al., 2012). The habenula receives afferent inputs from many forebrain regions (Bianco and Wilson, 2009), mediates reward-related behavior, and is linked to psychiatric disease (Li et al., 2011, 2013; Matsumoto and Hikosaka, 2007, 2009). It comprises two main subdomains: the medial habenula (mHb) and lateral habenula (lHb). The mHb primarily projects axons to the interpeduncular nucleus, while the lHb can directly innervate monoaminergic nuclei, including dopaminergic neurons (Bianco and Wilson, 2009; Hikosaka et al., 2008). The lHb is the only subdomain that receives reciprocal dopaminergic

innervation (Gruber et al., 2007), which acts as a feedback loop to inhibit lHb activity (Kowski et al., 2009; Shen et al., 2012; Stamatakis et al., 2013). However, our understanding of how subdomain-specific innervation patterns in the habenula and other brain nuclei are established is limited.

During development, axons rely not only on molecular gradients presented in the surrounding environment for guidance (Pasterkamp and Kolodkin, 2013) but also on signals provided by other axons (Grueber and Sagasti, 2010; Imai and Sakano, 2011; Luo and Flanagan, 2007; Tessier-Lavigne and Goodman, 1996; Wang and Marquardt, 2013). Axon-axon signaling serves critical roles in nervous system wiring, but the underlying mechanisms are incompletely understood. Furthermore, our current understanding of axon-axon interactions mainly derives from studies on axon types extending alongside as part of the same bundle. In contrast, molecular mechanisms that drive instructive interactions between reciprocally projecting axons, e.g., those between the habenula and dopamine system, and the contribution of such interactions to neural circuit assembly, remain largely unresolved. This is surprising, as reciprocal connections function as important feedback and feedforward loops in many neural circuits.

Here, we show that the habenula integrates different, previously uncharacterized cellular and molecular mechanisms to control its subdomain-specific innervation by dopaminergic axons. Our observations unveil a role for axon-axon signaling by showing that a specific subdomain, the lHb, sends out molecularly labeled efferent projections in a larger axon bundle to collect, sort, and guide its own reciprocal afferent projections in a subdomain-restricted manner. This process of subdomain-mediated axon-axon signaling cooperates with lHb-specific chemoattraction to control the specific innervation of the lHb by dopaminergic afferents. Together, our findings identify axonal wiring principles in the habenula that may also apply more generally to other brain nuclei or laminated structures.

RESULTS

The habenula receives subdomain-restricted afferent inputs, including those from dopaminergic neurons in the ventral tegmental area (VTA) (Figure 1A) (Gruber et al., 2007; Phillipson and Griffith, 1980). However, despite the important inhibitory role of these dopaminergic afferents on lHb activity (Stamatakis et al., 2013), how dopaminergic innervation of the habenula is established is unknown. To determine how dopaminergic afferents specifically innervate the lHb, we first characterized their ontogeny using immunohistochemistry for tyrosine hydroxylase (TH), the rate-limiting enzyme in dopamine synthesis. TH-positive axons started to project toward the habenula around E12.5 and arrived at this structure by E13.5. At E16.5, TH-positive axons had entered the lHb, but not the mHb, and 2 days later, at E18.5, this innervation was further increased (Figures 1B and 1C; data not shown). Thus, during development, dopaminergic axons selectively innervate the lHb without expanding into the mHb.

Netrin-1 Is a Subnucleus-Specific Attractant for Dopaminergic Axons

How is the selective innervation of the lHb achieved? To address this question, we searched for molecular differences between the mHb and lHb by using laser-capture microdissection in combination with mass spectrometry (Figure S1A available online). This analysis identified 2,880 unique proteins and revealed differential expression of several classes of proteins with established roles in neural circuit development, e.g., axon guidance and cell adhesion molecules (Table S1). A few of the identified proteins were shown previously to display lHb- or mHb-specific patterns of expression (Quina et al., 2009), confirming the specificity of the microdissection procedure. Analysis of the expression of several of the candidates revealed subdomain-specific expression for *Netrin-1* and *DCC* in the habenula. *DCC* strongly labeled the mHb at E16.5, while *Netrin-1* expression was confined to the lHb (Figure 1D). This pattern of *DCC* expression is in line with previous observations (Quina et al., 2009). Netrin-1 is a chemoattractant for dopaminergic axons via its DCC receptor (Cord et al., 2010; Lin et al., 2005; Xu et al., 2010), which has been detected throughout the embryonic and adult dopaminergic system (Cord et al., 2010; Lin et al., 2005; Manitt et al., 2013; Osborne et al., 2005; Xu et al., 2010). Indeed, immunohistochemistry showed DCC expression in dopaminergic afferents of the lHb, both at E16.5 (Figure S1B) and in the adult (Osborne et al., 2005).

The expression of DCC on dopaminergic axons en route to the lHb and *Netrin-1* in the lHb suggested that this ligand-receptor pair may regulate the dopaminergic innervation of this subnucleus. To test this model, we first performed explant coculture assays by combining VTA and lHb explants. Axons emanating from VTA explants preferentially extended toward lHb explants, and this effect was blocked by the addition of DCC function-blocking antibodies, but not immunoglobulin G (IgG) control antibodies (P/D ratio 1.39 ± 0.12 for control [n = 16 explants], 1.34 ± 0.09 for control IgG [n = 12 explants], and 1.01 ± 0.06 for anti-DCC [n = 10 explants]; $p < 0.05$; Figure S1C). Analysis of the trajectories of individual dopaminergic axons emerging parallel to the lHb explants (Figure S1D) (Bagnard et al., 1998; Pasterkamp et al., 2003) confirmed the ability of the lHb to reorient dopaminergic VTA axons in a DCC-dependent manner in vitro (Figure S1E). To establish that Netrin-1 can indeed attract dopaminergic axons projecting to the habenula, we developed an organotypic culture assay that recapitulates the in vivo development of the habenular system (Figure S2A) and positioned Netrin-1-expressing cells or control cells adjacent to the presumptive trajectory of the dopaminergic projections in E12.5 hemisections. Whereas the normal trajectory of dopaminergic axons toward the habenula was not affected by control cells, dopaminergic axons extending in the vicinity of Netrin-1-expressing cells were reoriented toward these cells (16.7% for control; 85.7% for Netrin-1, n = 6 and n = 7 slices for control and Netrin-1; $p < 0.05$; Figures 1E and 1G). To remove DCC from dopaminergic axons, *DCC* conditional mutants (Krimpenfort et al., 2012) were crossed with *Engrailed*(*En1*)*-Cre* mice, which drive Cre recombinase expression in the early embryonic midbrain, but not in the habenula (Figures S2B–S2E) (Kimmel et al., 2000). We tested several other Cre lines with reported expression in dopaminergic neurons (e.g., *Pitx3-Cre*, *DAT-Cre*), but none of these lines induced recombination at sufficiently early stages of development (data not shown). In cultures derived from *En1-Cre:DCC*$^{fl/fl}$ embryos, Netrin-1 cells could no

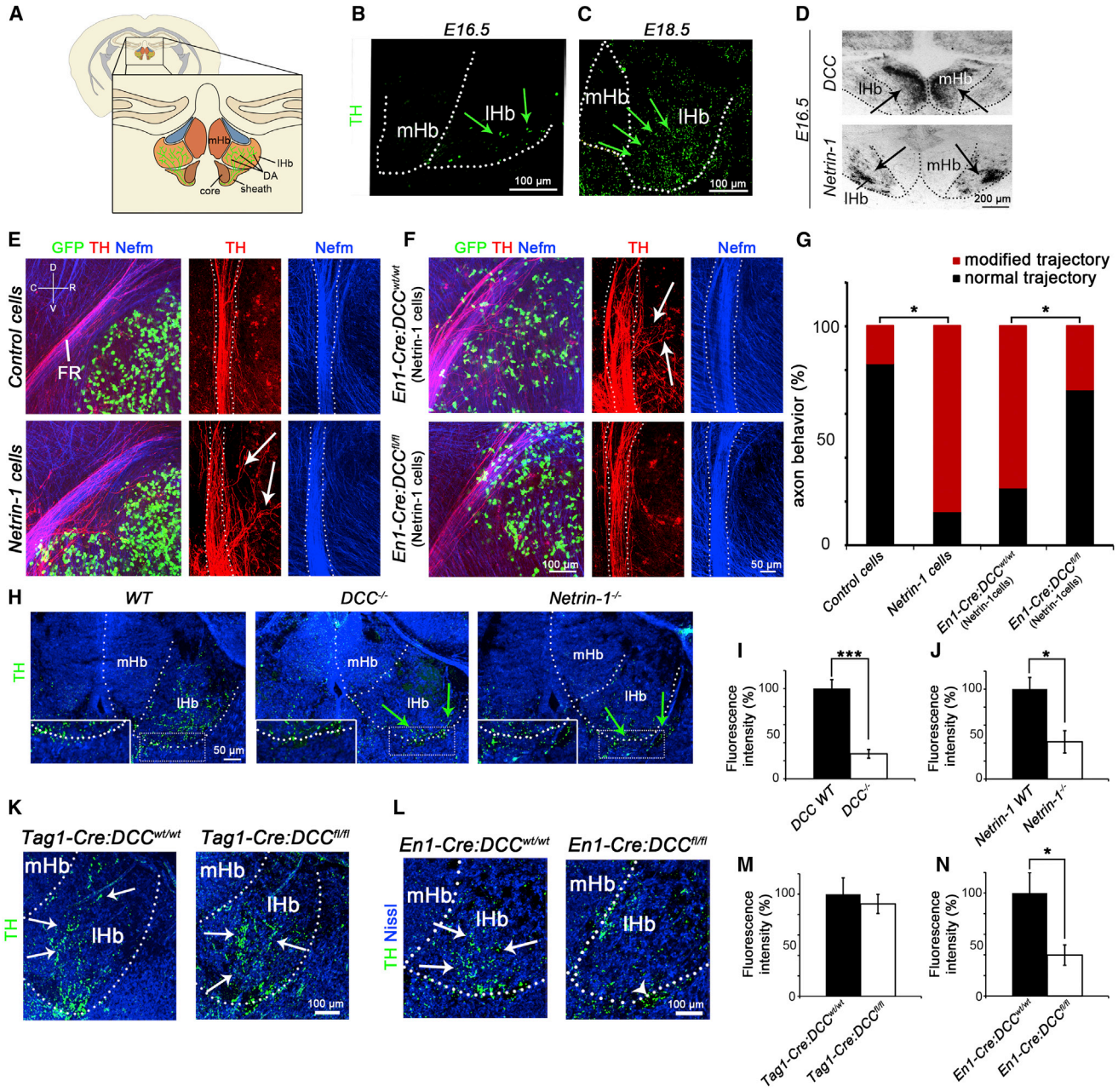

Figure 1. Netrin-1 Is a Subnucleus-Specific Attractant for Dopaminergic Axons

(A) Schematic of a coronal section of the mouse brain depicting the mHb, the lHb, and the FR. The FR is the major output bundle of the habenula. Dopaminergic (DA) innervation of the habenula is restricted to the lHb.

(B and C) Immunohistochemistry for TH on coronal sections of the embryonic habenula. Green arrows indicate TH-positive axons.

(D) In situ hybridization for *DCC* and *Netrin-1* in coronal sections of the habenula. Black arrows point to prominent expression of *DCC* in the mHb and of *Netrin-1* in the lHb.

(E and F) E12.5 organotypic slices were cultured for 3 days in vitro (DIV) and subjected to immunohistochemistry for GFP, TH, and Nefm. Placing Netrin-1-expressing cell aggregates adjacent to the presumptive FR reorients DA axons toward the aggregate (white arrows). This effect is not observed in cultures from *En1-Cre:DCC*$^{fl/fl}$ mice in which DCC is absent from DA neurons (F). C, caudal; D, dorsal; R, rostral; V, ventral.

(G) Quantification indicating the percentage of cultures with a normal or modified trajectory of dopaminergic projections. *$p < 0.05$.

(H) Immunohistochemistry for TH in coronal sections of the E18.5 habenula of WT, *DCC*$^{-/-}$, or *Netrin-1*$^{-/-}$ mice. Insets show a higher magnification of the boxed areas showing the ventral border of the lHb. Green arrows point to aberrant accumulation of dopaminergic axons.

(I and J) Quantification of the dopaminergic innervation of the lHb in *DCC*$^{-/-}$ (I) and *Netrin-1*$^{-/-}$ (J) mice. *$p < 0.05$, ***$p < 0.001$. Error bars indicate SEM.

(legend continued on next page)

longer significantly alter the normal linear trajectory of dopaminergic axons (73.3% for *En1-Cre:DCC*$^{wt/wt}$; 28.5% for *En1-Cre:DCC*$^{fl/fl}$, n = 15 and n = 7 slices for *En1-Cre:DCC*$^{wt/wt}$ and *En1-Cre:DCC*$^{fl/fl}$; $p < 0.05$; Figures 1F and 1G). Together, these data show that Netrin-1 secreted by the lHb acts as an attractant for DCC-expressing dopaminergic VTA axons.

Netrin-1 Controls Dopaminergic Axon Target Entry in the lHb

To examine whether DCC and Netrin-1 are required in vivo for subdomain-specific innervation of the lHb, dopaminergic targeting of the lHb was analyzed in *DCC*$^{-/-}$ and *Netrin-1*$^{-/-}$ mice at E18.5, when dopaminergic fibers occupy most of the lHb (Figure 1C). Genetic ablation of *DCC* resulted in an almost complete loss of lHb innervation (27.7% ± 4.8% of control, n = 4 mice for control and *DCC*$^{-/-}$; $p < 0.001$; Figures 1H and 1I), and TH-positive axons were found to accumulate at the ventral border of the lHb in *DCC*$^{-/-}$ mice instead of entering this structure (Figure 1H, insets). *Netrin-1*$^{-/-}$ mice displayed similar phenotypes, although some innervation of the lHb was observed, most likely because this mouse mutant is a hypomorph displaying residual Netrin-1 expression (41.3% ± 12.3% of control, n = 3 and n = 4 mice for control and *Netrin-1*$^{-/-}$, respectively; $p < 0.05$; Figures 1H and 1J) (Serafini et al., 1996). To determine whether lack of dopaminergic innervation of the lHb in *DCC*$^{-/-}$ mice is due to removal of DCC from habenular or dopaminergic axons, we next genetically ablated *DCC* in the habenula or in the dopaminergic midbrain. To remove DCC from the habenula, a bacterial artificial chromosome (BAC) mouse was generated expressing Cre recombinase under the control of *Tag-1* promotor sequences. Tag1 is a marker of the habenula, and *Tag-1-Cre:ROSA26-eYFP* mice revealed robust recombination in the habenula but not in dopaminergic neurons (Figure S3A). Crossing *Tag1-Cre* mice with *DCC*$^{fl/fl}$ mice resulted in loss of DCC expression in mHb neurons and axons (Figure S3B), but did not change the number of dopaminergic axons in the lHb (90.4% ± 9.4% of control, n = 3 mice; n.s.; Figures 1K and 1M). In contrast, loss of DCC in midbrain dopamine neurons in *En1-Cre:DCC*$^{fl/fl}$ mice caused reduced innervation of the lHb (39.7% ± 9.9% of control, n = 3 mice; $p < 0.05$; Figures 1L and 1N). This reduction was less severe in *En1-Cre:DCC*$^{fl/fl}$ mice as compared to *DCC* full knockout mice, presumably because En1 levels vary among dopaminergic neurons (Veenvliet et al., 2013). Nevertheless, the majority of dopaminergic axons accumulated at the lHb in *En1-Cre:DCC*$^{fl/fl}$ mice and did not enter the lHb (Figure 1L). Finally, we directed small interfering RNA (siRNA) targeting *Netrin-1* to the habenula at E12.5 before dopaminergic afferents reach this structure using ex vivo electroporation (Figure S3C). Electroporation with Netrin-1 siRNAs induced a significant decrease in the dopaminergic innervation of the lHb (Figures S3D–S3G). This effect was evident despite our observation that only a subset of habenular neurons is targeted by the ex vivo electroporation procedure. Collectively, these data show that Netrin-1 expressed in the lHb instructs dopaminergic axons expressing DCC to enter the lHb (Figure S3H).

Reciprocal Axon-Axon Interactions Guide Dopaminergic Afferents to the lHb

Although dopaminergic axons did reach the lHb in *DCC*$^{-/-}$ and *Netrin-1*$^{-/-}$ mice, we observed that their organization in the fasciculus retroflexus (FR) was severely disrupted. The FR is the major output bundle of the habenula, in which efferent habenular axons are intermingled with specific afferent projections. Habenular efferents display a characteristic segregated distribution in the FR, with axons from the mHb projecting in the core of the bundle, and lHb axons forming a sheath around this core (Figure 2A) (Bianco and Wilson, 2009). To analyze this organization in relation to dopaminergic afferents in *DCC*$^{-/-}$ and *Netrin-1*$^{-/-}$ mice, we identified and applied new markers for mHb and lHb axons: Robo3 and neurofilament medium polypeptide (Nefm), respectively (Figure S4A). In E18.5 wild-type (WT) mice, TH-positive axons were restricted to the Nefm-positive sheath region and absent from the Robo3-positive core (Figures 2B and S4A). In contrast, in *DCC*$^{-/-}$ and *Netrin-1*$^{-/-}$ mice, thick bundles of TH-positive axons traversed the entire width of the FR (Figure 2B). The mutant FR consisted mainly of Nefm-positive axons, while only a few Robo3-positive axons were detected. Instead, an aberrant population of Robo3-positive mHb axons was detected at the dorsal roof of the habenula (Figure S4B). These results, together with the ability of Netrin-1 to attract habenular axons in vitro, and DCC and *Netrin-1* expression in the FR core and ventral midbrain, respectively (Funato et al., 2000), suggest that Netrin-1 and DCC are required for the guidance of mHb axons to the midbrain. Interestingly, TH-positive axons in the FR in *DCC*$^{-/-}$ and *Netrin-1*$^{-/-}$ mice were restricted to regions occupied by Nefm-positive lHb axons, resembling their close association in the sheath region of WT mice. Furthermore, the overall number of TH-positive axons reaching the lHb in mutant mice was comparable to control (data not shown). Ablation of DCC in the habenula in *Tag1-Cre:DCC*$^{fl/fl}$ mice induced similar phenotypes, namely, intermingling of the TH and lHb axons throughout the width of the FR and a dorsal redirection of many Robo3-positive mHb axons (Figures 2C, 2D, and S4C). In contrast, loss of DCC in dopaminergic axons in *En1-Cre:DCC*$^{fl/fl}$ mice did not affect the organization of the FR (Figures 2E and 2F). Together, these data suggest that dopaminergic axons utilize lHb efferents to reach the lHb (Figure 2G). This latter hypothesis is in line with our observation that during development, habenular axons first extend to the ventral midbrain, following which, dopaminergic axons reciprocally project to the habenula along the developing FR (Figure S5).

To evaluate a model in which dopaminergic axons use lHb efferents to reach the lHb, and to study whether such dependency would be uni- or bidirectional, we performed in vivo genetic ablation studies. DTA mice, which conditionally express subunit A of the diphtheria toxin, were crossed with *Tag1-Cre*

(K and L) Immunohistochemistry for TH in coronal sections of E18.5 *Tag1-Cre:DCC*$^{wt/wt}$ and *Tag1-Cre:DCC*$^{fl/fl}$ mice (K) or *En1-Cre:DCC*$^{wt/wt}$ and *En1-Cre:DCC*$^{fl/fl}$ mice (L). White arrows indicate dopaminergic axons in the lHb. Arrowhead in (L) indicates accumulation of dopaminergic axons at the ventral border of the lHb. (M and N) Quantification of the dopaminergic innervation of the lHb in *Tag1-Cre:DCC* (M) and *En1-Cre:DCC* (N) conditional knockout mice. Innervation is not affected in *Tag1-Cre:DCC*$^{fl/fl}$ mice, but is dramatically reduced in *En1-Cre:DCC*$^{fl/fl}$ mice. *$p < 0.05$. Error bars indicate SEM. See also Figures S1, S2, and Table S1.

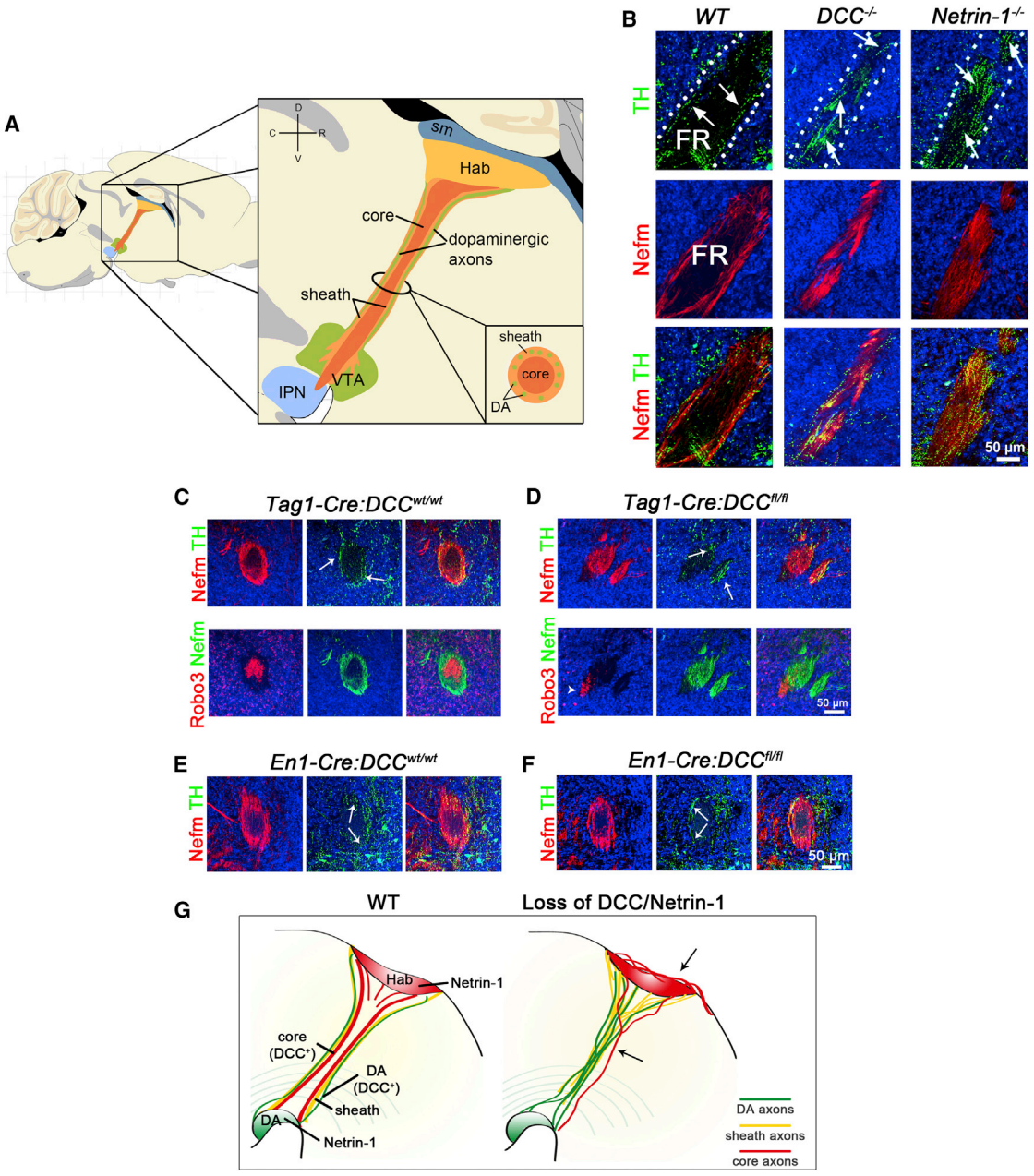

Figure 2. Abnormal Organization of the FR in *DCC* and *Netrin-1* Knockout Mice

(A) Schematic of a sagittal section of the mouse brain showing the segregated organization of habenular (Hab) and dopaminergic axons in the FR. Axons from mHb neurons run in the core of the FR, while lHb and dopaminergic (DA) axons are closely associated in the sheath of the FR. IPN, interpeduncular nucleus; sm, stria medullaris; VTA, ventral tegmental area.

(B) Double immunohistochemistry for TH and Nefm on sagittal sections. In E18.5 *DCC* and *Netrin-1* knockout mice, thick bundles of TH-positive axons and Nefm-positive habenular axons intermingle throughout the entire FR (arrows), contrasting their normal lateral distribution in the FR in WT (arrows) mice.

(C and D) Immunohistochemistry for Robo3, Nefm, and TH on coronal sections of the FR of E18.5 *Tag1-Cre:DCC* conditional knockout mice. The organization of the FR is severely disrupted in *Tag1-Cre:DCC*$^{fl/fl}$ mice: TH-positive axons intermingle with lHb axons throughout the FR (arrow), while a small number of Robo3-positive mHb axons are situated outside of the sheath (arrowhead).

(E and F) Immunohistochemistry for Nefm and TH on coronal sections of the FR of E18.5 *En1-Cre:DCC* conditional knockout mice.

(G) Schematic representation of the disrupted organization of the FR following loss of Netrin-1 or DCC. Misrouted core axons are observed at the dorsal roof of the habenula, and closely associated lHb and dopaminergic axons occupy the entire FR (arrows). In the absence of Netrin-1/DCC signaling, dopaminergic afferents do not enter the lHb and core axons fail to extend toward the midbrain. See also Figures S3 and S4.

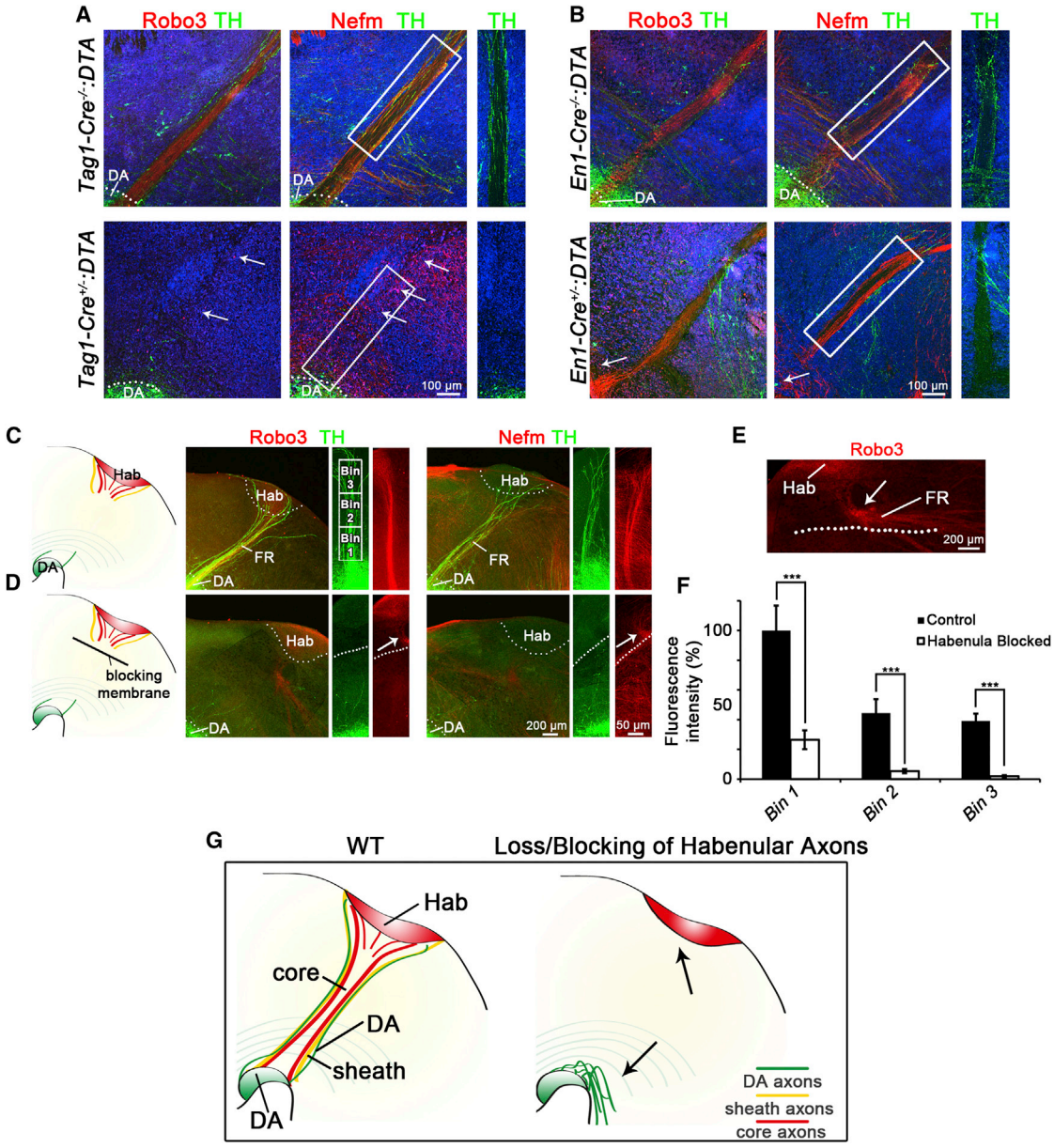

Figure 3. IHb Axons Serve as a Scaffold for Dopaminergic Afferents Targeting This Subnucleus

(A and B) Immunohistochemistry for Nefm, Robo3, and/or TH on sagittal sections of E18.5 *Tag1-Cre:DTA* and *En1-Cre:DTA* mice. The FR is absent in *Tag1-Cre*$^{+/-}$*:DTA* mice (A), (white arrows) and TH-positive dopaminergic (DA) axons fail to project to the habenula (A). In *En1-Cre*$^{+/-}$*:DTA* mice, midbrain DA neurons are absent (white arrows), but the FR is intact (B). Boxed areas are shown at a higher magnification at the right.

(C–E) E12.5 organotypic slices were cultured for 3 DIV and subjected to immunohistochemistry for Robo3, TH, and Nefm. Insertion of blocking membranes (dotted lines) redirects habenular axons (white arrows, magnification in E) and prevents growth of DA axons toward the habenula (D). Squares in (C) show bins used for quantification shown in (F).

(F) Growth of DA axons was quantified using the bins shown in (C). All bins were normalized to Bin 1 of the control condition. ***$p < 0.001$. Error bars indicate SEM.

(G) Schematic representation of the effect of Hab and FR ablation or of insertion of blocking membranes on dopaminergic axon growth toward the Hab. See also Figures S5 and S6.

mice to ablate the habenula. *Tag1-Cre:DTA* embryos displayed a loss of the habenula and the FR, whereas dopaminergic neurons in the VTA were unaffected (Figures S6A–S6E). No dopaminergic projections extended to the habenula in *Tag1-Cre:DTA* mice, while other dopaminergic pathways in the brain were intact (Figures 3A and S6C). Thus, dopaminergic axons require the habenula and/or the FR for guidance toward the IHb. To assess whether the converse, IHb axons depending on dopaminergic neurons or axons for guidance to the midbrain, is true, the region of the midbrain containing dopaminergic neurons was ablated

by crossing *En1-cre* and *DTA* mice. Although *En1-cre:DTA* embryos showed complete loss of midbrain dopaminergic neurons and their axons, the projection and organization of mHb and lHb neurons and axons were intact (Figures 3B, S6F, and S6G).

Together, these data reveal that dopaminergic axons are dependent on either long-distance instructive cues from the habenula or short-range cues on lHb axons in the sheath for long-distance guidance to the lHb. To investigate these two possibilities, we placed a blocking membrane at the ventral border of the habenula in E12.5 mouse brain hemisections and cultured them for 3 days. The membrane contains pores that allow the diffusion of secreted molecules but block the growth of axons (López-Bendito et al., 2006). In cultures without membrane insertion, a clear FR had formed with both mHb and lHb axons extending into the midbrain, as visualized by Robo3 and Nefm immunohistochemistry in combination with TH staining (Figure 3C). In contrast, insertion of blocking membranes prevented the extension of the FR to the midbrain (Figures 3D and 3E). In addition, the number of dopaminergic axons growing to the habenula was dramatically reduced (Bin1, 26.4% ± 6.3% of control; Bin2, 44.4% ± 9.3% for control, and 5.3% ± 1.4% for blocked, n = 7 and n = 10 slices for control and blocked; $p < 0.001$; Figures 3C–3F), and no dopaminergic axons were detected directly at the habenula (Bin3, 39.1% ± 2.8% for control and 1.9% ± 0.4% for blocked; $p < 0.001$; Figures 3C–3F). Thus, our expression, genetic, and cell culture data show that dopaminergic axons depend on short-range cues on lHb axons for guidance toward the lHb (Figure 3G). This suggests that the lHb sends out efferent projections to collect and guide its own afferent projections.

Subdomain-Specific Axon Guidance and Cell Adhesion Molecule Expression in the FR

Although our data show that dopaminergic projections rely on lHb axons for guidance toward the habenula, how this interaction is mediated at the molecular level is not known. To identify the underlying molecular mechanism, laser-capture microdissection experiments were performed on the embryonic FR in combination with mass spectrometry analysis to identify subdomain-specific proteins in the FR at the time of dopaminergic axon pathfinding (Figure 4A). Since axon guidance proteins and adhesion molecules are likely candidates for mediating axon-axon interactions, these proteins were selected from the mass spectrometry data and subjected to immunohistochemical analysis (Table S2; Figures 4B–4D). Immunohistochemistry on transverse sections of the FR showed that these selected proteins can be grouped on basis of their subdomain localization within the FR. Candidates were either localized to the entire FR (Figure 4B), the core (Figure 4C), or the sheath domain (Figure 4D). These results reveal subdomain-specific expression of various axon guidance and cell adhesion molecules in the developing FR, uncovering a molecular code that could underlie various aspects of FR organization, including the segregation of different axonal populations and their guidance toward specific subdomains.

Axon-Derived LAMP Guides Dopaminergic Axons to the lHb

Two FR proteins identified by mass spectrometry (Table S2) displayed sheath-specific expression; close homolog of L1 (CHL1) and limbic-system-associated protein (LAMP) (Figure 4D). Given their selective expression and reported role in cell adhesion and neurite outgrowth (Hillenbrand et al., 1999; Zhukareva and Levitt, 1995), we next assessed whether CHL1 or LAMP mediated interactions between lHb and dopaminergic axons. CHL1 is a type I transmembrane protein, while LAMP is tethered to the membrane via a glycosylphosphatidylinositol (GPI) anchor. We exploited these differences in membrane presentation by using the enzyme phosphatidylinositol-specific phospholipase C (PI-PLC) in combination with hemisection cultures. PI-PLC will remove GPI-linked proteins, such as LAMP, but leaves transmembrane proteins, such as CHL1, intact (Figure 5A). Treatment with PI-PLC did not affect the initial growth of TH-positive axons toward the habenula, indicating that this enzymatic treatment does not have a deleterious effect on axon growth (Bin1, 102.9% ± 16.23% of control, n = 11 slices for control and PI-PLC; $p = 0.896$; Figures 5B and 5C). Despite this initial growth toward the habenula, dopaminergic axons did not reach this brain region following PI-PLC treatment, but rather stalled or detached from the FR halfway along their normal trajectory (Bin2, 82.8% ± 12.2% for control and 45% ± 7.8% for PI-PLC; $p < 0.05$; Bin3, 63.1% ± 7.4% for control and 15% ± 2.3% for PI-PLC; $p < 0.001$; Figures 5B and 5C). PI-PLC treatment did not alter the growth of Nefm-positive habenular axons in the FR (Figure 5B).

To confirm that the impaired growth of TH-positive axons toward the habenula following PI-PLC application resulted from the cleavage of LAMP, LAMP function-blocking antibodies were applied to the hemisection cultures (Figure 5D). In line with the effect of PI-PLC treatment (Figures 5A–5C), TH-positive axon growth toward the habenula was reduced, with many axons running off the FR in the presence of anti-LAMP antibodies (Bin1, 70.4% ± 4.3% of control, n = 15 and n = 17 slices for control and anti-LAMP; $p < 0.001$; Bin2, 61.9% ± 4.9% for control and 35.1% ± 4.3% for anti-LAMP; $p < 0.001$; Bin3, 48.3% ± 3.32% for control and 23.3% ± 3% for anti-LAMP; $p < 0.001$; Figures 5E and 5F). Application of PI-PLC induced a greater reduction of TH-positive axons as compared to anti-LAMP antibody application. This could reflect an inability of the antibody to block all LAMP, perhaps due to limited tissue penetration or a role for additional GPI-linked proteins in the development of dopaminergic projections to the lHb. Anti-LAMP antibody treatment did not alter the growth of habenular axons in the FR (Figure 5E).

LAMP is a member of the IgLON family, which includes proteins that promote or inhibit cell adhesion and axon growth of specific neuronal populations (Gil et al., 2002; Keller et al., 1989; Zhukareva and Levitt, 1995). Therefore, we hypothesized that LAMP on lHb axons serves as an adhesive and growth-promoting substrate for dopaminergic axons. To test this idea, dopaminergic explant cultures were grown on coverslips coated with control or LAMP substrate. In line with the PI-PLC and antibody-blocking experiments, TH-positive axon growth was increased on LAMP as compared to control protein (116.1% ± 3.24% of control, n = 310 and n = 320 neurites for control and LAMP; $p < 0.001$; Figures 6A and 6B). To examine whether LAMP is not only a growth-promoting but also an instructive cue for dopaminergic axons, we cultured VTA explants on

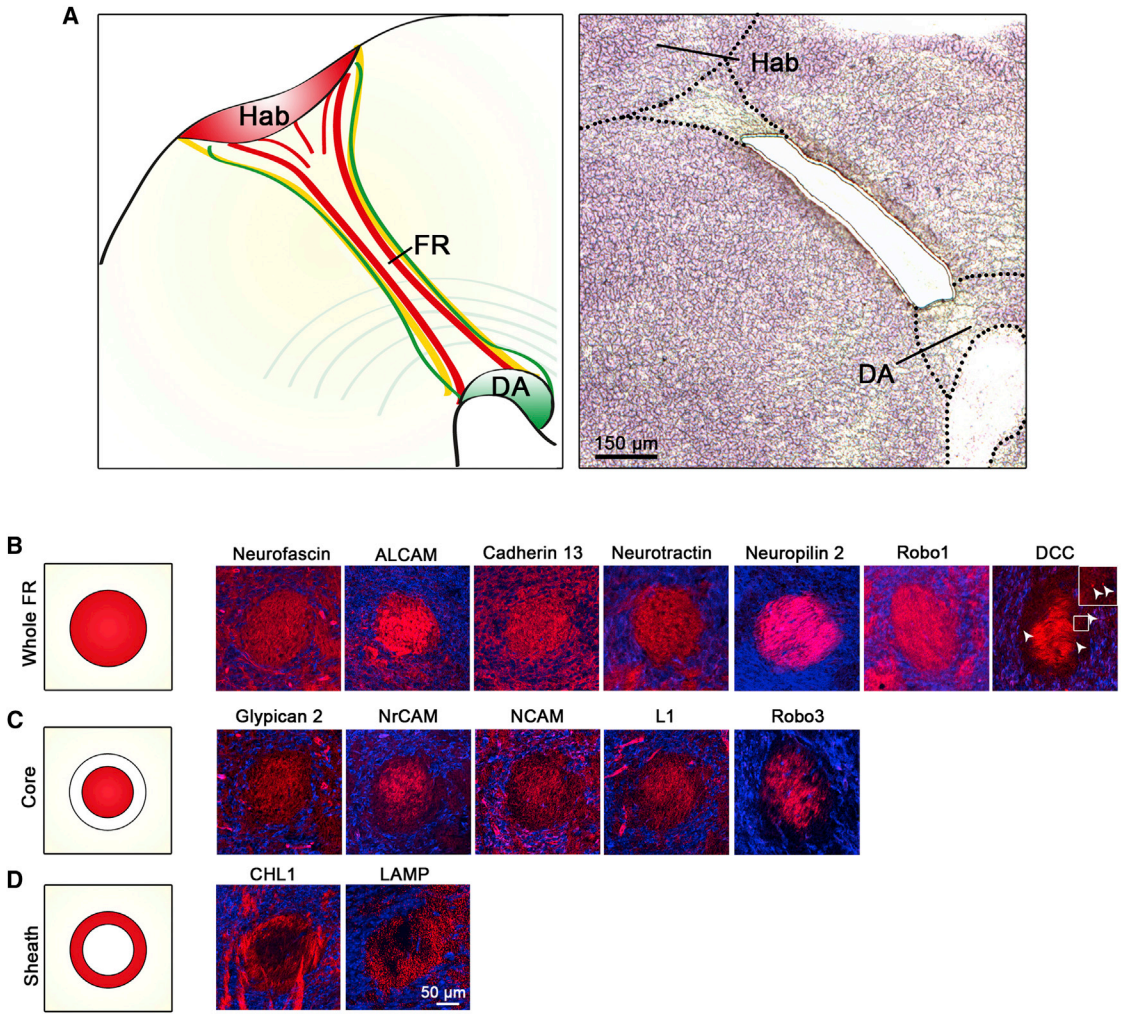

Figure 4. Laser-Capture Microdissection of the FR Reveals Subdomain-Specific Expression of Axon Guidance and Cell Adhesion Molecules

(A) Laser-capture microdissection was performed on the FR in E16.5 sagittal mouse brain sections. Hab, habenula; DA, dopamine neuron pool.

(B–D) Immunohistochemistry on coronal sections of the FR using antibodies against different axon guidance and cell adhesion molecules. Proteins identified by mass spectrometry on FR samples display three modes of expression: throughout the FR (B), restricted to the core region of the FR (C), or specific to the sheath (D). Inset in (B) shows a magnification of the indicated boxed area. DCC-positive axons (white arrowheads) are located in the sheath of the FR. See also Table S2.

alternating stripes of control and LAMP protein or on control stripes only. Control stripes had no effect on dopaminergic axons extending from the explants. In contrast, dopaminergic axons displayed a clear preference for LAMP stripes when provided with a choice between control and LAMP substrate (157% ± 18.8% of control, n = 52 explants for LAMP and control; $p < 0.05$; Figures 6C and 6D). Together, these experiments show that LAMP serves as a growth-promoting and instructive cue for dopaminergic VTA axons.

To confirm the specificity of the antibody experiments and to establish that LAMP expressed by lHb axons, rather than other structures in the vicinity of the FR, guides dopaminergic axons, we directed siRNAs to the habenula during early stages of dopaminergic pathfinding using ex vivo electroporation. siRNAs were introduced at E12.5 or E13.5, followed by immunohistochemical assessment of the trajectories of habenular and dopaminergic axons 3 days later. Electroporation with scrambled control siRNAs did not visibly alter the growth or trajectory of habenular or dopaminergic axons. In contrast, LAMP knockdown induced a significant decrease in the outgrowth of TH-positive axons toward the habenula, causing a marked reduction in the dopaminergic innervation of this nucleus (Bin3, 82.6% ± 7.5% for control [n = 13 slices] and 52% ± 8.5% [n = 8 slices] for si-LAMP; $p < 0.05$; Figures 6G–6I, and S7A–S7D). Furthermore, similar to our observations following PI-PLC treatment and antibody application, many TH-positive axons detached from the FR halfway along their trajectory toward the habenula (Figure 6H). LAMP knockdown did not visibly alter the growth of Nefm-positive habenular axons in the FR (Figures 6G and 6H).

To show that LAMP not only guides dopaminergic afferents to the lHb but also has an instructive role in the targeting

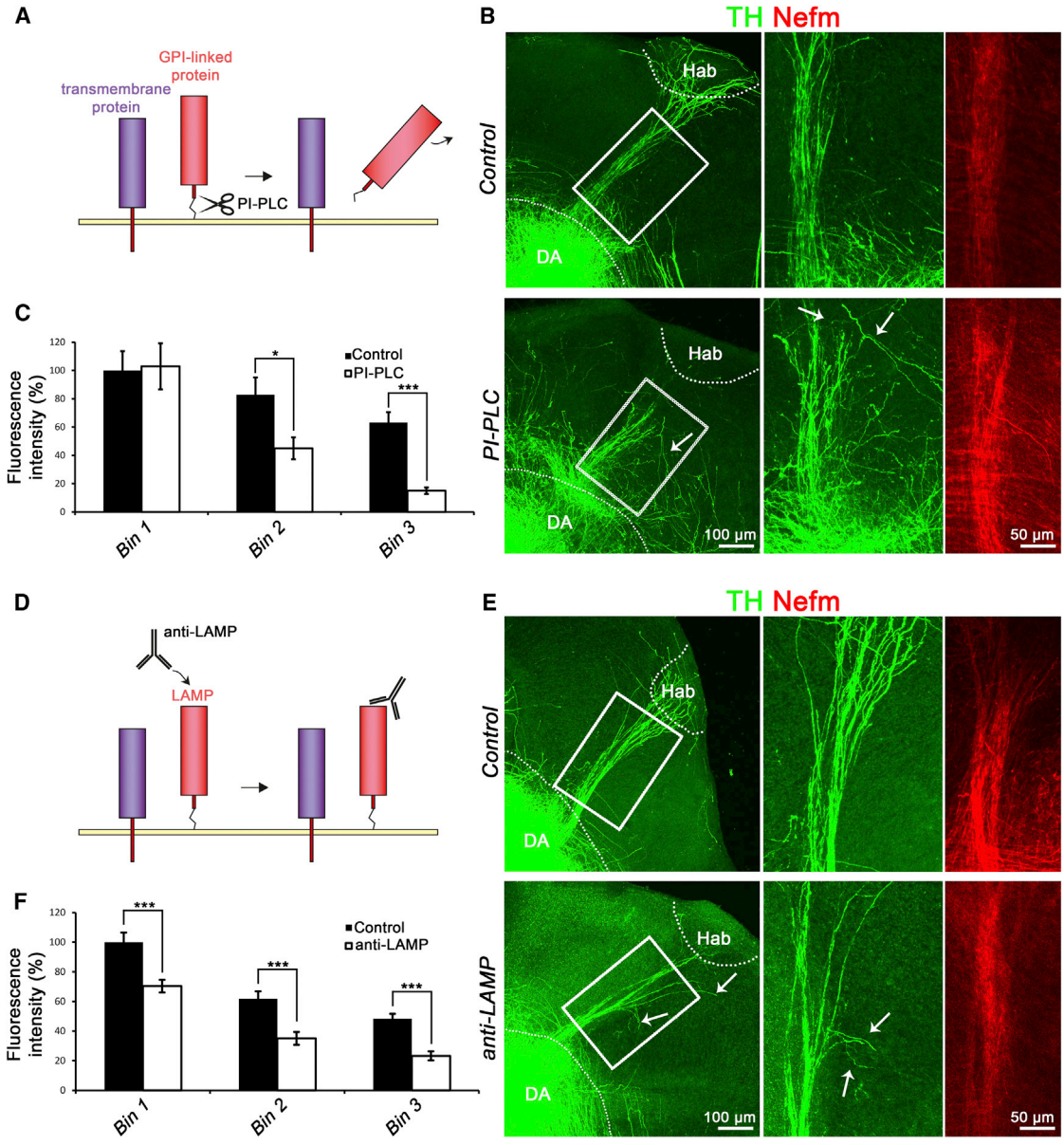

Figure 5. The GPI-Linked Cell Adhesion Molecule LAMP Mediates Guidance of Dopaminergic Axons to the Habenula

(A and D) Schematics showing the PI-PLC or function-blocking antibody treatments to specifically remove GPI-anchored molecules (A) or block LAMP (D).

(B and E) Immunohistochemistry for TH and Nefm on E12.5 organotypic slice cultures treated with PI-PLC or anti-LAMP antibodies and cultured for 3 DIV. Boxed areas are shown at higher magnification in two right panels. White arrows indicate stalled or detached axons. DA, dopaminergic; Hab, habenula.

(C and F) Quantification of PI-PLC or antibody-treated cultures using bins as shown in Figure 3C. *$p < 0.05$, ***$p < 0.001$. Error bars indicate SEM.

dopaminergic axons specifically toward the lHb, we ectopically expressed LAMP in the mHb or in a region adjacent to the lHb and FR using ex vivo electroporation. Coelectroporation of LAMP and GFP expression vectors confirmed the presence of LAMP protein in electroporated neurons and axons (Figure S7E). LAMP or control expression vectors were electroporated at E13.5 and dopaminergic innervation of the FR and habenula was assessed 3 days later. As expected, in experiments targeting the habenula, many GFP-positive neurons were present in the mHb and extended axons into the core of the FR. Interestingly, TH-positive axons from the sheath region often crossed over to nearby GFP/LAMP-positive axons in the core but never to axons expressing GFP only (Figure 7A). This effect was also reflected at the level of the mHb. Robo3 was used to identify the mHb, which was devoid of dopaminergic axons after electroporation of GFP (Figures 7B and S7F). In contrast, overexpression of GFP and LAMP induced aberrant dopaminergic innervation of the mHb (321.4% ± 70.8% of control, n = 11 and n = 14 slices for control and LAMP, respectively; $p < 0.05$; Figures 7B and 7C). Although only a small subset of

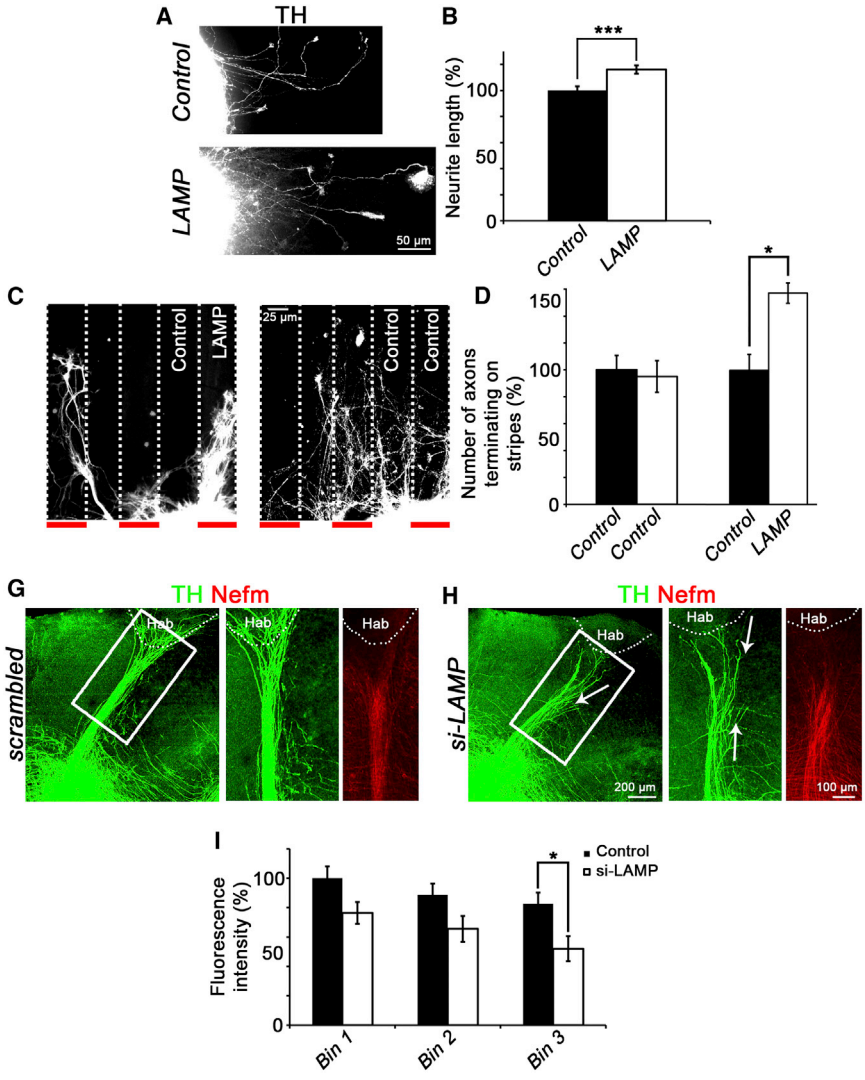

Figure 6. LAMP Mediates Growth of Dopaminergic Afferents toward the Habenula

(A and B) Explants of the E14.5 VTA were grown on control or LAMP substrate and subjected to immunocytochemistry for TH (A). The length of TH-positive axons is increased on LAMP as compared to control substrate (B). ***$p < 0.001$. Error bars denote SEM.

(C and D) Explants of the E14.5 VTA were grown on alternating control and LAMP stripes or on control stripes only, and subjected to immunohistochemistry for TH (C). Axons show a preference for growth on LAMP stripes over control stripes (D). *$p < 0.05$. Error bars denote SEM.

(G and H) Immunohistochemistry for TH and Nefm following electroporation of the habenula with scrambled (G) or *LAMP* (H) siRNAs. White arrows indicate detached axons.

(I) Quantification of fluorescence intensity using bins as shown in Figure 3C. *$p < 0.05$. Error bars denote SEM. See also Figure S7.

mHb neurons was targeted by the ex vivo electroporation procedure, several dopaminergic axons were found to abnormally innervate the mHb along GFP-positive axons and continue along the cell bodies and processes of LAMP-expressing neurons in the mHb (Figure 7B). Ectopic expression of LAMP adjacent to the lHb or the FR had no effect on the trajectory of TH-positive or habenular axons. TH-positive axons followed the FR into the lHb but did not extend into adjacent regions of ectopic LAMP expression (n = 4 slices; Figure 7D). Thus, LAMP functions on lHb axons to direct dopaminergic axons to the lHb. Finally, to examine whether LAMP is required in vivo for the innervation of the lHb by dopaminergic afferents, *LAMP*$^{-/-}$ embryos were analyzed (Innos et al., 2011). In line with the antibody-blocking and siRNA-induced knockdown experiments (Figures 5D, 5E, and 6G–6I), genetic ablation of *LAMP* caused a marked reduction in the dopaminergic innervation of the lHb at E18.5 (Figures 7E and 7F, n = 4 mice for WT and *LAMP*$^{-/-}$). Furthermore, many TH-positive axons detached from the FR in *LAMP*$^{-/-}$ embryos and invaded the region immediately surrounding this bundle, resembling the detachment of dopaminergic axons observed following manipulation of LAMP ex vivo (Figures 7E and 7G). The ability of a subset of dopaminergic axons to innervate the lHb in the absence of LAMP may reflect compensation by other proteins. No defects in the trajectories of habenular efferents were observed in *LAMP*$^{-/-}$ embryos (Figure 7G). Together, these results show that LAMP expressed on lHb axons in the sheath of the FR serves as a molecular scaffold for dopaminergic axons, guiding these axons to a specific subdomain of the habenula: the lHb (Figures 7H and 7I). These data indicate that pretarget reciprocal axon-axon signaling can contribute to subdomain-specific axon targeting and provide insight into the function of the poorly characterized IgCAM LAMP.

DISCUSSION

Numerous brain nuclei are distinguishable in the vertebrate nervous system, and often these structures are further subdivided on a functional basis into smaller subdomains. Although clustering of neurons into (sub)nuclei facilitates the generation of highly specific patterns of synaptic connectivity, how brain nuclei are formed and innervated remains poorly understood. Here we show that reciprocal axon-axon interactions cooperate with subnucleus-restricted chemoattractive mechanisms to coordinate the dopaminergic innervation of the lateral subnucleus of the lHb. We demonstrate that the lHb determines its own pattern of afferent innervation by sending out LAMP-positive efferent projections that reciprocally guide dopaminergic afferents to the lHb. At the lHb, the secreted attractant Netrin-1 is

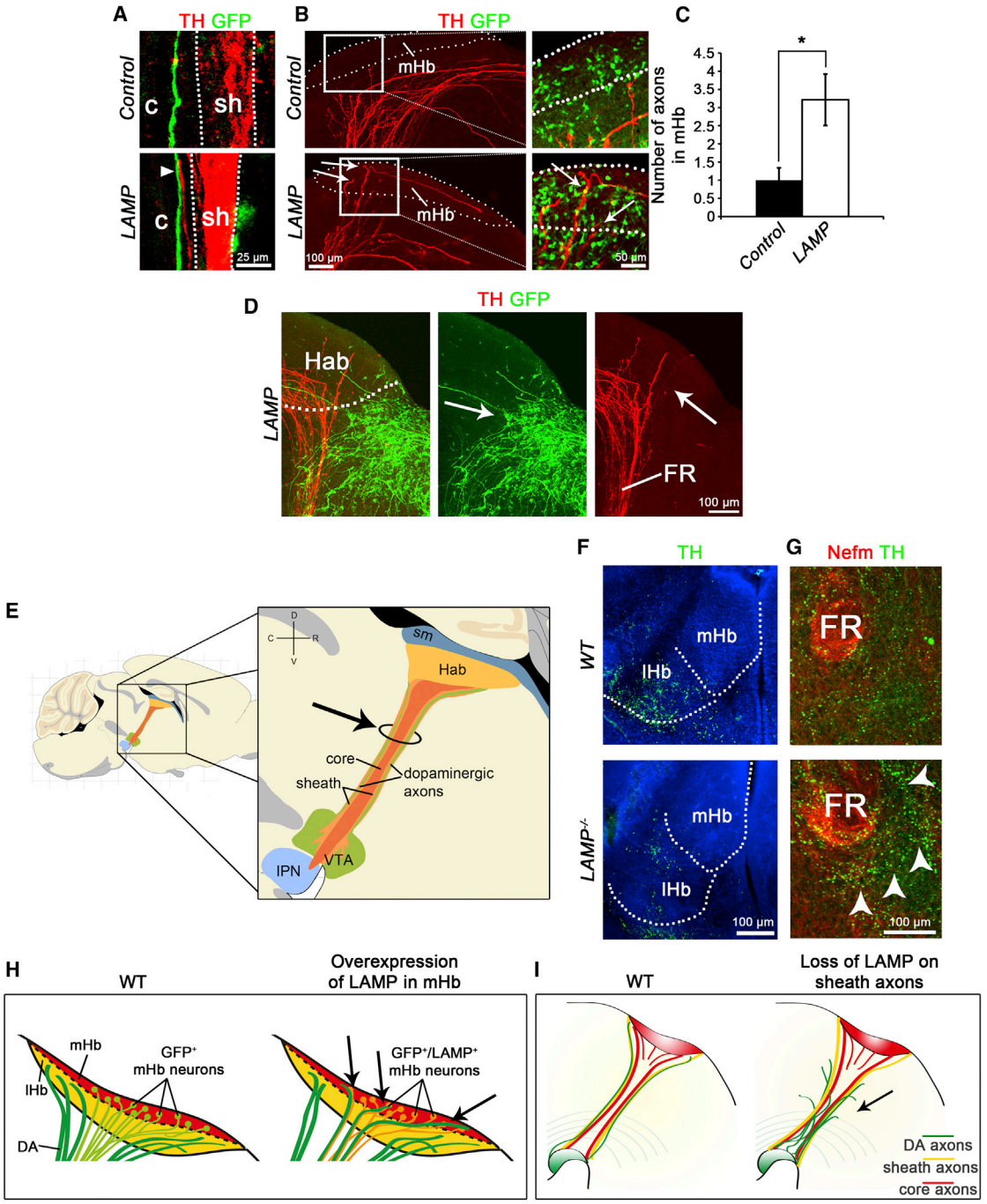

Figure 7. LAMP Is Required on lHb Axons to Establish Subdomain-Restricted Innervation of the Habenula by Dopaminergic Afferents

(A and B) Immunohistochemistry for TH and GFP on slice cultures 3 days after electroporation. Dotted lines in (A) indicate sheath region and arrowhead points to a TH-positive axon crossing over from the sheath region to a GFP/ LAMP-positive core axon. c, core; sh, sheath. Dotted line in (B) indicates the mHb as determined by immunohistochemistry for Robo3. Boxed area is shown at higher magnification at the right. Arrows indicate TH-positive axons extending along GFP/LAMP-expressing cell bodies and processes in the mHb.

(C) Quantification of the number of dopaminergic axons innervating the mHb. *$p < 0.05$. Error bars denote SEM.

(D) Immunohistochemistry for TH and GFP on slice cultures 3 days after electroporation. Dotted line in (D) indicates the habenula (Hab). Ectopic expression of LAMP adjacent to the habenula does not induce misrouting of TH-positive axons. FR, fasciculus retroflexus.

(E) Schematic of a sagittal section of the mouse brain showing the segregated organization of habenular (Hab) and dopaminergic axons in the FR. Black arrow indicates the position of the coronal section in (G). IPN, interpeduncular nucleus; sm, stria medullaris; VTA, ventral tegmental area.

(legend continued on next page)

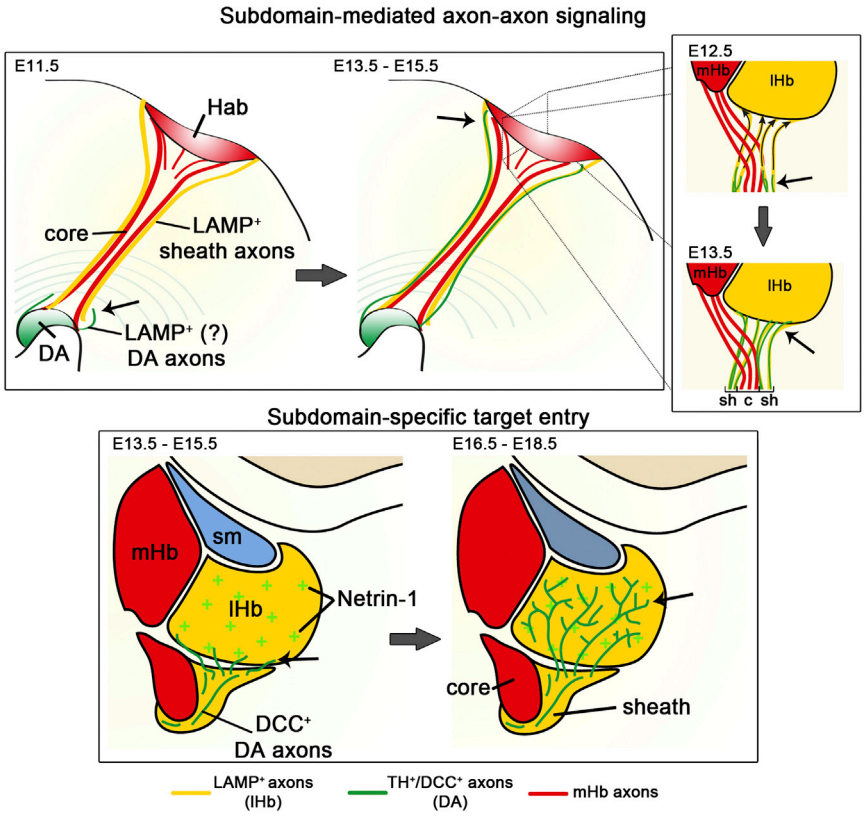

Figure 8. Subdomain-Specific Innervation of the Habenula Requires Cooperation between Reciprocal Axon-Axon Signaling and Subnucleus-Restricted Chemoattraction

In our model, the lateral subnucleus of the lHb sends out efferent projections that selectively express the cell adhesion molecule LAMP to reciprocally guide afferent dopaminergic (DA) axons over a long distance and deliver these axons specifically to the border of the lHb, a process we refer to as subdomain-mediated axon-axon signaling. At the lHb, subdomain-restricted expression of the secreted attractant Netrin-1 is required for the entry of DCC-expressing dopaminergic afferents into this subnucleus. See text for more details. c, core; Hab, habenula; mHb, medial habenula; lHb, lateral habenula; sh, sheath; sm, stria medullaris.

required for the entry of dopaminergic afferents into this subnucleus (Figure 8). Together, our findings identify pretarget axon-axon signaling mediated by axonal cues derived from the target as a mechanism to wire reciprocally connected brain regions in a subdomain-specific manner.

Reciprocal Axon-Axon Signaling Guides Dopaminergic Afferents

Although the guidance of axons by chemotropic cues in their environment has been well established (Pasterkamp and Kolodkin, 2013), less is known about the role of axon-derived cues. It is clear, however, that axon-axon interactions are used to establish complex neural circuits (Grueber and Sagasti, 2010; Imai and Sakano, 2011; Luo and Flanagan, 2007; Tessier-Lavigne and Goodman, 1996; Wang and Marquardt, 2013). Our knowledge of these interactions mainly derives from studies on interactions between subgroups of axons extending alongside in the same direction within large bundles. For example, Eph-ephrin signaling between sensory and motor axons in the periphery mediates their segregation and guidance (Gallarda et al., 2008; Wang et al., 2011), while axon-derived semaphorins and their receptors mediate pretarget sorting of olfactory sensory axons (Imai et al., 2009; Joo et al., 2013; Lattemann et al., 2007). How interactions between reciprocally projecting axon types are controlled or contribute to circuit assembly is poorly understood.

The habenula is an excellent system for studying axon-axon signaling. Neurons in the lHb and mHb give rise to well-characterized, anatomically segregated efferent projections in a large axon bundle: the FR. In addition, during early development, many habenular afferents make a binary choice between the lHb and mHb, providing a sensitive assay for studies on axon target selection and innervation. Finally, the habenular system not only contains efferent and afferent axon types that run alongside in the same direction, but also harbors reciprocal connections (Figure 2A) (Bianco and Wilson, 2009). Here we exploited these characteristics to reveal a requirement for reciprocal axon-axon signaling in the development of subdomain-specific dopaminergic connections. Remarkably, our data show that the lHb determines its own pattern of afferent innervation by sending out molecularly labeled efferents in a larger axon bundle that collect, sort, and guide afferents and specifically deliver them to the lHb, a phenomenon we term subdomain-mediated axon-axon signaling (Figure 8). Multiple lines of evidence support this model. First, expression data localize dopaminergic axons in the FR sheath intermingled with reciprocally projecting lHb axons. Second, dopaminergic axon targeting of the lHb is largely intact in *Tag1-Cre:DCC*$^{fl/fl}$ mice in which the FR is almost exclusively composed of lHb axons. Third, blockage of habenular axon growth in vitro and genetic ablation of the habenula and the FR in vivo prevents dopaminergic innervation of the lHb. Fourth, neutralization, knockdown, or knockout

(F and G) Immunohistochemistry for TH and Nefm on coronal sections of the habenula and FR of E18.5 WT or *LAMP*$^{-/-}$ mice. Loss of LAMP results in a reduction of dopaminergic innervation of the lHb (F). In addition, rather than extending in the FR sheath, many TH-positive axons traverse the region surrounding the FR in *LAMP*$^{-/-}$ mice (G) (arrowheads).

(H and I) Schematics summarizing the effects of ectopic LAMP expression, LAMP knockdown, or knockout on dopaminergic axon guidance toward the habenula and on subdomain targeting in the habenula. See also Figure S7.

of the lHb-specific cue LAMP prevents dopaminergic innervation of the lHb. Finally, ectopic LAMP expression in mHb neurons and their axons erroneously redirects dopaminergic afferents to the mHb.

One of the best-studied examples of reciprocal axon-axon interactions is the interdependency of thalamocortical and corticothalamic axons (Molnár et al., 2012). During development, thalamocortical axons traverse the subpallium and are then used by corticothalamic afferents for reciprocal guidance through this intermediate target (Deck et al., 2013). However, whether these reciprocal axon-axon interactions also contribute to the subdomain-specific innervation of the cortex or thalamus, and which axonal cues mediate these interactions, is unknown. Our data show that reciprocal axon-axon interactions not only provide a scaffold for guidance, but also function to direct afferent projections to specific subdomains within the target. Further, our study provides an example of a protein that can mediate such reciprocal axon-axon interactions: LAMP. LAMP is an instructive cue for dopaminergic axons and is expressed in dopaminergic neurons that project afferents to the habenula (Figures 7A–7D and S7G). This, together with the fact that the adhesive effects of LAMP are attributed to homophilic interactions (Zhukareva and Levitt, 1995), supports a model in which homophilic LAMP interactions guide dopaminergic axons (Figure 8). Notably, LAMP is also expressed in reciprocally connected parts of the thalamus and cortex, and in vitro it regulates the growth and guidance of the axonal projections connecting these structures (Mann et al., 1998). Further studies are needed to determine whether LAMP mediates interactions between thalamocortical and corticothalamic axons, or other reciprocal connections in the brain, analogous to its role in the habenular system.

Axon-Axon Signaling Regulates Subdomain-Specific Axon Targeting

The ordered distribution of different axon types in large axon tracts is a pervasive anatomical feature of neural circuits and underlies the generation of precise synaptic connections (Wang and Marquardt, 2013). Efferent projections from the mHb and lHb are segregated in the core and sheath regions of the FR, respectively. Although the molecular basis of this segregation is unknown, our findings show that lHb axon-derived LAMP localizes dopaminergic afferents to the FR sheath. In addition, misexpression of LAMP in the mHb and core axons aberrantly redirects dopaminergic afferents to the mHb, revealing that LAMP-positive lHb axons not only guide dopaminergic afferents but also dictate their subdomain targeting. Our current understanding of the molecular basis of subdomain-specific axon targeting mainly derives from studies on laminar structures, such as the hippocampus and the visual system. This work shows that target-derived guidance cues first direct axons toward or away from specific laminae followed by the combinatorial expression of cell adhesion molecules, which facilitates the formation of (sub)lamina-specific synaptic contacts (Baier, 2013; Huberman et al., 2010; Robles and Baier, 2012; Sanes and Yamagata, 2009; Williams et al., 2010). Our data show that subdomain-mediated axon-axon signaling provides an additional strategy to regulate subdomain-specific circuit assembly that relies on axon-axon interactions rather than on cues expressed in the target. Previous studies have implicated axon-axon signaling in different aspects of target selection, innervation, and mapping (Imai et al., 2009; Lattemann et al., 2007; Mizumoto and Shen, 2013; Schwabe et al., 2013; Sweeney et al., 2007; Takeuchi et al., 2010). Our findings are, however, conceptually distinct from these previous reports: we find that molecular interactions between reciprocal, efferent, and afferent axons target dopaminergic afferents to the lHb, rather than signaling between afferent projections heading for the same target. Thus, while previous work has shown pretarget axon-axon signaling independent from the target, our work now identifies a role for axonally expressed cues generated by neurons in the target in the subdomain-specific guidance of afferent axons.

Netrin-1 Is a Subdomain-Specific Cue Regulating Subnuclear Axon Target Entry

Although one might predict that dopaminergic axons would simply follow LAMP-positive axons into the lHb to meet their synaptic targets, our data identify a requirement for Netrin-1 in the entry of dopaminergic afferents into this subnucleus (Figure 8). In the absence of Netrin-1, or its receptor DCC, dopaminergic axons accumulate at their normal entry site of the lHb. Our data show that Netrin-1 secreted by the lHb serves as an attractant for DCC-expressing dopaminergic axons en route to the lHb. Analysis of conditional and full *DCC* and *Netrin-1* mutant mice suggests that in vivo Netrin-1 most likely functions as a short-range attractant, since axons arrive at the lHb in the absence of Netrin-1-DCC signaling but accumulate at its ventral border. This idea is in line with recent work on short-range attractive effects of Netrin-B during the lamina-specific targeting of R8 retinal axons in the medulla of the *Drosophila* optic lobe (Timofeev et al., 2012). Here, Netrin-B is released in the R8 axon-recipient layer M3 of the retina by afferent axonal projections and subsequently captured by neuron-associated Frazzled; the fly homolog of DCC. This results in a short-range Netrin-B signal that attracts ingrowing R8 axons into layer M3. Our data extend these findings by showing that Netrin-1 mediates the entry of dopaminergic afferents into a specific subnucleus in vertebrate species. This indicates that Netrins play conserved roles in the subdomain-specific innervation of both laminated structures and brain nuclei, and identifies a role for these cues distinct from previously reported functions in, for example, axon guidance, topographic sorting, and synaptogenesis (Bielle et al., 2011; Goldman et al., 2013; Lai Wing Sun et al., 2011; Manitt et al., 2011; Poon et al., 2008; Powell et al., 2008; and references therein).

Our work further shows that at least two distinct mechanisms are needed to control the dopaminergic innervation of the lHb. A possible explanation for this cooperation between axon-axon signaling and chemoattraction is that lHb axons act to deliver dopaminergic axons specifically at the lHb, following which, Netrin-1 uncouples these axons. This would allow other (non)axonal molecular signals within the lHb to guide dopaminergic axons to their partner neurons. Further studies will be needed to dissect the mechanistic details of Netrin-1-mediated axon target entry.

Despite its important physiological functions and its implication in disorders such as major depressive disorder (MDD) (Hikosaka, 2010), the mechanisms underlying habenular circuit

development in mammals remain largely unknown (Chen et al., 2000; Funato et al., 2000; Giger et al., 2000; Kantor et al., 2004). Our study reveals mechanisms that enable the generation of highly specific patterns of afferent innervation of the habenula. These principles may apply not only to dopaminergic axons but also to the many other afferent projections targeting the habenula (Bianco and Wilson, 2009). Together, our work provides tools and a conceptual framework for the further dissection of habenular circuit assembly. More generally, our findings unveil an unexpected cooperation between subdomain-mediated axon-axon signaling and subnucleus-restricted chemoattraction in subdomain-specific axon targeting. Analogous combinatorial targeting strategies could be widely used because many brain nuclei and layered structures in the nervous system display subdomain-specific patterns of guidance-cue expression and are interconnected with their afferent target regions though reciprocal axon projections.

EXPERIMENTAL PROCEDURES

Mouse Lines

Animal use and care was in accordance with local institutional guidelines. Generation of transgenic mice and all other mouse lines used in this study are described in the Supplemental Experimental Procedures.

Immunohistochemistry and In Situ Hybridization

Nonradioactive in situ hybridization and immunohistochemistry were performed as described previously (Kolk et al., 2009; Pasterkamp et al., 2007). Average fluorescence intensity was measured using the histogram function in Adobe Photoshop. Background was determined in areas without staining and subtracted from images, after which mean signal intensity was determined.

Laser-Capture Microdissection

Laser-capture microdissection was performed using a PALM laser microscope system (Zeiss). Samples were subjected to SDS-PAGE and were sent for mass spectrometry analysis.

Explant and Organotypic Slice Cultures

3D collagen matrix assays were performed as described previously (Schmidt et al., 2012). See Supplemental Experimental Procedures for a detailed description of the antibody preparation, coating, and quantification. For organotypic slice cultures, E12.5 mouse brains were dissected to produce two sagittal hemisections. Following 3 days in culture, hemisections were fixed in 4% PFA and stained using appropriate antibodies.

Ex Vivo Electroporation

For electroporation, mouse embryos were collected at E12.5 or E13.5, and the third ventricle was injected with siRNA (25 μM) and DNA (1 μg/μl). After electroporation, hemisections were cultured as described above for the organotypic slice cultures. To test siRNA knockdown efficiency, (1) HEK293 cells were plated onto poly-D-lysine-coated coverslips. siRNAs (ON-TARGET plus SMARTpool; Dharmacon) were transfected using Lipofectamine 2000 (Invitrogen) according to manufacturer's protocol, and (2) the E14–E15 cerebral cortex was electroporated with siRNAs, cultured, and analyzed by quantitative PCR.

Quantification and Statistics Methods

Statistical analyses were performed using IBM SPSS Statistics by Student's t test or chi-square test (for hemisection-aggregate assays). All data in this manuscript are derived from at least three independently performed experiments. All data were expressed as means ± SEM, and significance was defined as $p < 0.05$.

SUPPLEMENTAL INFORMATION

Supplemental Information includes seven figures, two tables, and Supplemental Experimental Procedures and can be found with this article online at http://dx.doi.org/10.1016/j.neuron.2014.05.036.

ACKNOWLEDGMENTS

We thank members of the R.J.P. laboratory for assistance and discussions and Alex Kolodkin and Guillermina Lopez-Bendito for reading the manuscript. We thank Marc Tessier-Lavigne, Anton Berns, Cecilia Flores, Wolfgang Wurst, Alain Chedotal, Meng Li, Seji Miyata, and Helen Cooper for sharing reagents and mice. We thank Nicoletta Kessaris and Jerre van Veluw for advice and technical assistance. Anti-Tag1 and anti-LAMP antibodies were obtained from the Developmental Studies Hybridoma Bank. This study is supported by grants from the Netherlands Organization for Scientific Research (TopTalent; to E.R.E.S.), Stichting Parkinson Fonds, the Netherlands Organization for Health Research and Development (VIDI, ZonMW-TOP), the European Union (mdDANeurodev, FP7/2007-2011, Grant 222999), and the People Programme (Marie Curie Actions) of the European Union's Seventh Framework Programme FP7/2007-2013/under REA grant agreement number [289581] (NPlast) (to R.J.P.). This study was partly performed within the framework of Dutch Top Institute Pharma Project T5-207 (to R.J.P.). This work was partly supported by project grants (631466 and 1043045) from the National Health and Medical Research Council, Australia (NHMRC). L.J.R. was supported by an NHMRC Principal Research fellowship, A.-L.S.D was supported by an Australian Post-graduate Award scholarship and a top-up scholarship from the QBI, and E.V. was supported by an Institutional investigation grant (IUT20-41) from the Estonian Research Council.

Accepted: May 21, 2014
Published: July 16, 2014

REFERENCES

Aizawa, H., Kobayashi, M., Tanaka, S., Fukai, T., and Okamoto, H. (2012). Molecular characterization of the subnuclei in rat habenula. J. Comp. Neurol. *520*, 4051–4066.

Bagnard, D., Lohrum, M., Uziel, D., Püschel, A.W., and Bolz, J. (1998). Semaphorins act as attractive and repulsive guidance signals during the development of cortical projections. Development *125*, 5043–5053.

Baier, H. (2013). Synaptic laminae in the visual system: molecular mechanisms forming layers of perception. Annu. Rev. Cell Dev. Biol. *29*, 385–416.

Bianco, I.H., and Wilson, S.W. (2009). The habenular nuclei: a conserved asymmetric relay station in the vertebrate brain. Philos. Trans. R. Soc. Lond. B Biol. Sci. *364*, 1005–1020.

Bielle, F., Marcos-Mondéjar, P., Leyva-Díaz, E., Lokmane, L., Mire, E., Mailhes, C., Keita, M., García, N., Tessier-Lavigne, M., Garel, S., and López-Bendito, G. (2011). Emergent growth cone responses to combinations of Slit1 and Netrin 1 in thalamocortical axon topography. Curr. Biol. *21*, 1748–1755.

Chen, H., Bagri, A., Zupicich, J.A., Zou, Y., Stoeckli, E., Pleasure, S.J., Lowenstein, D.H., Skarnes, W.C., Chédotal, A., and Tessier-Lavigne, M. (2000). Neuropilin-2 regulates the development of selective cranial and sensory nerves and hippocampal mossy fiber projections. Neuron *25*, 43–56.

Cord, B.J., Li, J., Works, M., McConnell, S.K., Palmer, T., and Hynes, M.A. (2010). Characterization of axon guidance cue sensitivity of human embryonic stem cell-derived dopaminergic neurons. Mol. Cell. Neurosci. *45*, 324–334.

Deck, M., Lokmane, L., Chauvet, S., Mailhes, C., Keita, M., Niquille, M., Yoshida, M., Yoshida, Y., Lebrand, C., Mann, F., et al. (2013). Pathfinding of corticothalamic axons relies on a rendezvous with thalamic projections. Neuron *77*, 472–484.

Funato, H., Saito-Nakazato, Y., and Takahashi, H. (2000). Axonal growth from the habenular nucleus along the neuromere boundary region of the diencephalon is regulated by semaphorin 3F and netrin-1. Mol. Cell. Neurosci. *16*, 206–220.

Gallarda, B.W., Bonanomi, D., Müller, D., Brown, A., Alaynick, W.A., Andrews, S.E., Lemke, G., Pfaff, S.L., and Marquardt, T. (2008). Segregation of axial motor and sensory pathways via heterotypic trans-axonal signaling. Science *320*, 233–236.

Giger, R.J., Cloutier, J.F., Sahay, A., Prinjha, R.K., Levengood, D.V., Moore, S.E., Pickering, S., Simmons, D., Rastan, S., Walsh, F.S., et al. (2000). Neuropilin-2 is required in vivo for selective axon guidance responses to secreted semaphorins. Neuron *25*, 29–41.

Gil, O.D., Zhang, L., Chen, S., Ren, Y.Q., Pimenta, A., Zanazzi, G., Hillman, D., Levitt, P., and Salzer, J.L. (2002). Complementary expression and heterophilic interactions between IgLON family members neurotrimin and LAMP. J. Neurobiol. *51*, 190–204.

Goldman, J.S., Ashour, M.A., Magdesian, M.H., Tritsch, N.X., Harris, S.N., Christofi, N., Chemali, R., Stern, Y.E., Thompson-Steckel, G., Gris, P., et al. (2013). Netrin-1 promotes excitatory synaptogenesis between cortical neurons by initiating synapse assembly. J. Neurosci. *33*, 17278–17289.

Gruber, C., Kahl, A., Lebenheim, L., Kowski, A., Dittgen, A., and Veh, R.W. (2007). Dopaminergic projections from the VTA substantially contribute to the mesohabenular pathway in the rat. Neurosci. Lett. *427*, 165–170.

Grueber, W., and Sagasti, A. (2010). Self-avoidance and tiling: mechanisms of dendrite and axon spacing. Cold Spring Harb. Perspect. Biol. *2*, a001750.

Hikosaka, O. (2010). The habenula: from stress evasion to value-based decision-making. Nat. Rev. Neurosci. *11*, 503–513.

Hikosaka, O., Sesack, S.R., Lecourtier, L., and Shepard, P.D. (2008). Habenula: crossroad between the basal ganglia and the limbic system. J. Neurosci. *28*, 11825–11829.

Hillenbrand, R., Molthagen, M., Montag, D., and Schachner, M. (1999). The close homologue of the neural adhesion molecule L1 (CHL1): patterns of expression and promotion of neurite outgrowth by heterophilic interactions. Eur. J. Neurosci. *11*, 813–826.

Huberman, A.D., Clandinin, T.R., and Baier, H. (2010). Molecular and cellular mechanisms of lamina-specific axon targeting. Cold Spring Harb. Perspect. Biol. *2*, a001743.

Imai, T., and Sakano, H. (2011). Axon-axon interactions in neuronal circuit assembly: lessons from olfactory map formation. Eur. J. Neurosci. *34*, 1647–1654.

Imai, T., Yamazaki, T., Kobayakawa, R., Kobayakawa, K., Abe, T., Suzuki, M., and Sakano, H. (2009). Pre-target axon sorting establishes the neural map topography. Science *325*, 585–590.

Innos, J., Philips, M.A., Leidmaa, E., Heinla, I., Raud, S., Reemann, P., Plaas, M., Nurk, K., Kurrikoff, K., Matto, V., et al. (2011). Lower anxiety and a decrease in agonistic behaviour in Lsamp-deficient mice. Behav. Brain Res. *217*, 21–31.

Joo, W.J., Sweeney, L.B., Liang, L., and Luo, L. (2013). Linking cell fate, trajectory choice, and target selection: genetic analysis of Sema-2b in olfactory axon targeting. Neuron *78*, 673–686.

Kantor, D.B., Chivatakarn, O., Peer, K.L., Oster, S.F., Inatani, M., Hansen, M.J., Flanagan, J.G., Yamaguchi, Y., Sretavan, D.W., Giger, R.J., and Kolodkin, A.L. (2004). Semaphorin 5A is a bifunctional axon guidance cue regulated by heparan and chondroitin sulfate proteoglycans. Neuron *44*, 961–975.

Keller, F., Rimvall, K., Barbe, M.F., and Levitt, P. (1989). A membrane glycoprotein associated with the limbic system mediates the formation of the septo-hippocampal pathway in vitro. Neuron *3*, 551–561.

Kimmel, R.A., Turnbull, D.H., Blanquet, V., Wurst, W., Loomis, C.A., and Joyner, A.L. (2000). Two lineage boundaries coordinate vertebrate apical ectodermal ridge formation. Genes Dev. *14*, 1377–1389.

Kolk, S.M., Gunput, R.A., Tran, T.S., van den Heuvel, D.M.A., Prasad, A.A., Hellemons, A.J., Adolfs, Y., Ginty, D.D., Kolodkin, A.L., Burbach, J.P.H., et al. (2009). Semaphorin 3F is a bifunctional guidance cue for dopaminergic axons and controls their fasciculation, channeling, rostral growth, and intracortical targeting. J. Neurosci. *29*, 12542–12557.

Kowski, A.B., Veh, R.W., and Weiss, T. (2009). Dopaminergic activation excites rat lateral habenular neurons in vivo. Neuroscience *161*, 1154–1165.

Krimpenfort, P., Song, J.-Y., Proost, N., Zevenhoven, J., Jonkers, J., and Berns, A. (2012). Deleted in colorectal carcinoma suppresses metastasis in p53-deficient mammary tumours. Nature *482*, 538–541.

Lai Wing Sun, K., Correia, J.P., and Kennedy, T.E. (2011). Netrins: versatile extracellular cues with diverse functions. Development *138*, 2153–2169.

Lattemann, M., Zierau, A., Schulte, C., Seidl, S., Kuhlmann, B., and Hummel, T. (2007). Semaphorin-1a controls receptor neuron-specific axonal convergence in the primary olfactory center of *Drosophila*. Neuron *53*, 169–184.

Li, B., Piriz, J., Mirrione, M., Chung, C., Proulx, C.D., Schulz, D., Henn, F., and Malinow, R. (2011). Synaptic potentiation onto habenula neurons in the learned helplessness model of depression. Nature *470*, 535–539.

Li, K., Zhou, T., Liao, L., Yang, Z., Wong, C., Henn, F., Malinow, R., Yates, J.R., III, and Hu, H. (2013). βCaMKII in lateral habenula mediates core symptoms of depression. Science *341*, 1016–1020.

Lin, L., Rao, Y., and Isacson, O. (2005). Netrin-1 and slit-2 regulate and direct neurite growth of ventral midbrain dopaminergic neurons. Mol. Cell. Neurosci. *28*, 547–555.

López-Bendito, G., Cautinat, A., Sánchez, J.A., Bielle, F., Flames, N., Garratt, A.N., Talmage, D.A., Role, L.W., Charnay, P., Marín, O., and Garel, S. (2006). Tangential neuronal migration controls axon guidance: a role for neuregulin-1 in thalamocortical axon navigation. Cell *125*, 127–142.

Luo, L., and Flanagan, J.G. (2007). Development of continuous and discrete neural maps. Neuron *56*, 284–300.

Manitt, C., Mimee, A., Eng, C., Pokinko, M., Stroh, T., Cooper, H.M., Kolb, B., and Flores, C. (2011). The netrin receptor DCC is required in the pubertal organization of mesocortical dopamine circuitry. J. Neurosci. *31*, 8381–8394.

Manitt, C., Eng, C., Pokinko, M., Ryan, R.T., Torres-Berrío, A., Lopez, J.P., Yogendran, S.V., Daubaras, M.J., Grant, A., Schmidt, E.R., et al. (2013). dcc orchestrates the development of the prefrontal cortex during adolescence and is altered in psychiatric patients. Transcult. Psychiatry *3*, e338.

Mann, F., Zhukareva, V., Pimenta, A., Levitt, P., and Bolz, J. (1998). Membrane-associated molecules guide limbic and nonlimbic thalamocortical projections. J. Neurosci. *18*, 9409–9419.

Matsumoto, M., and Hikosaka, O. (2007). Lateral habenula as a source of negative reward signals in dopamine neurons. Nature *447*, 1111–1115.

Matsumoto, M., and Hikosaka, O. (2009). Representation of negative motivational value in the primate lateral habenula. Nat. Neurosci. *12*, 77–84.

Mizumoto, K., and Shen, K. (2013). Interaxonal interaction defines tiled presynaptic innervation in C. elegans. Neuron *77*, 655–666.

Molnár, Z., Garel, S., López-Bendito, G., Maness, P., and Price, D.J. (2012). Mechanisms controlling the guidance of thalamocortical axons through the embryonic forebrain. Eur. J. Neurosci. *35*, 1573–1585.

Osborne, P.B., Halliday, G.M., Cooper, H.M., and Keast, J.R. (2005). Localization of immunoreactivity for deleted in colorectal cancer (DCC), the receptor for the guidance factor netrin-1, in ventral tier dopamine projection pathways in adult rodents. Neuroscience *131*, 671–681.

Pasterkamp, R.J., and Kolodkin, A.L. (2013). SnapShot: axon guidance. Cell *153*, 494.

Pasterkamp, R.J., Peschon, J.J., Spriggs, M.K., and Kolodkin, A.L. (2003). Semaphorin 7A promotes axon outgrowth through integrins and MAPKs. Nature *424*, 398–405.

Pasterkamp, R.J., Kolk, S.M., Hellemons, A.J.C.G.M., and Kolodkin, A.L. (2007). Expression patterns of semaphorin7A and plexinC1 during rat neural development suggest roles in axon guidance and neuronal migration. BMC Dev. Biol. *7*, 98.

Phillipson, O.T., and Griffith, A.C. (1980). The neurones of origin for the mesohabenular dopamine pathway. Brain Res. *197*, 213–218.

Poon, V.Y., Klassen, M.P., and Shen, K. (2008). UNC-6/netrin and its receptor UNC-5 locally exclude presynaptic components from dendrites. Nature *455*, 669–673.

Powell, A.W., Sassa, T., Wu, Y., Tessier-Lavigne, M., and Polleux, F. (2008). Topography of thalamic projections requires attractive and repulsive functions of Netrin-1 in the ventral telencephalon. PLoS Biol. *6*, e116.

Quina, L.A., Wang, S., Ng, L., and Turner, E.E. (2009). Brn3a and Nurr1 mediate a gene regulatory pathway for habenula development. J. Neurosci. *29*, 14309–14322.

Robles, E., and Baier, H. (2012). Assembly of synaptic laminae by axon guidance molecules. Curr. Opin. Neurobiol. *22*, 799–804.

Sanes, J.R., and Yamagata, M. (2009). Many paths to synaptic specificity. Annu. Rev. Cell Dev. Biol. *25*, 161–195.

Schmidt, E.R.E., Morello, F., and Pasterkamp, R.J. (2012). Dissection and culture of mouse dopaminergic and striatal explants in three-dimensional collagen matrix assays. J. Vis. Exp. http://dx.doi.org/10.3791/3691.

Schwabe, T., Neuert, H., and Clandinin, T.R. (2013). A network of cadherin-mediated interactions polarizes growth cones to determine targeting specificity. Cell *154*, 351–364.

Serafini, T., Colamarino, S.A., Leonardo, E.D., Wang, H., Beddington, R., Skarnes, W.C., and Tessier-Lavigne, M. (1996). Netrin-1 is required for commissural axon guidance in the developing vertebrate nervous system. Cell *87*, 1001–1014.

Shen, X., Ruan, X., and Zhao, H. (2012). Stimulation of midbrain dopaminergic structures modifies firing rates of rat lateral habenula neurons. PLoS ONE *7*, e34323.

Stamatakis, A.M., Jennings, J.H., Ung, R.L., Blair, G.A., Weinberg, R.J., Neve, R.L., Boyce, F., Mattis, J., Ramakrishnan, C., Deisseroth, K., and Stuber, G.D. (2013). A unique population of ventral tegmental area neurons inhibits the lateral habenula to promote reward. Neuron *80*, 1039–1053.

Sweeney, L.B., Couto, A., Chou, Y.-H., Berdnik, D., Dickson, B.J., Luo, L., and Komiyama, T. (2007). Temporal target restriction of olfactory receptor neurons by Semaphorin-1a/PlexinA-mediated axon-axon interactions. Neuron *53*, 185–200.

Takeuchi, H., Inokuchi, K., Aoki, M., Suto, F., Tsuboi, A., Matsuda, I., Suzuki, M., Aiba, A., Serizawa, S., Yoshihara, Y., et al. (2010). Sequential arrival and graded secretion of Sema3F by olfactory neuron axons specify map topography at the bulb. Cell *141*, 1056–1067.

Tessier-Lavigne, M., and Goodman, C.S. (1996). The molecular biology of axon guidance. Science *274*, 1123–1133.

Timofeev, K., Joly, W., Hadjieconomou, D., and Salecker, I. (2012). Localized netrins act as positional cues to control layer-specific targeting of photoreceptor axons in Drosophila. Neuron *75*, 80–93.

Veenvliet, J.V., Dos Santos, M.T., Kouwenhoven, W.M., von Oerthel, L., Lim, J.L., van der Linden, A.J.A., Koerkamp, M.J.G., Holstege, F.C.P., and Smidt, M.P. (2013). Specification of dopaminergic subsets involves interplay of En1 and Pitx3. Development *140*, 3373–3384.

Wang, L., and Marquardt, T. (2013). What axons tell each other: axon-axon signaling in nerve and circuit assembly. Curr. Opin. Neurobiol. *23*, 974–982.

Wang, L., Klein, R., Zheng, B., and Marquardt, T. (2011). Anatomical coupling of sensory and motor nerve trajectory via axon tracking. Neuron *71*, 263–277.

Williams, M.E., de Wit, J., and Ghosh, A. (2010). Molecular mechanisms of synaptic specificity in developing neural circuits. Neuron *68*, 9–18.

Xu, B., Goldman, J.S., Rymar, V.V., Forget, C., Lo, P.S., Bull, S.J., Vereker, E., Barker, P.A., Trudeau, L.E., Sadikot, A.F., and Kennedy, T.E. (2010). Critical roles for the netrin receptor deleted in colorectal cancer in dopaminergic neuronal precursor migration, axon guidance, and axon arborization. Neuroscience *169*, 932–949.

Zhukareva, V., and Levitt, P. (1995). The limbic system-associated membrane protein (LAMP) selectively mediates interactions with specific central neuron populations. Development *121*, 1161–1172.